Pergamon

Journal of Structural Geology, Vol. 20, No. 9/10, pp. 1247 to 1259, 1998

0191-8141/98/$ - see front matter

PII: S0191-8141(98)00065-0

Emplacement and deformation of granites during transpression: magnetic fabrics of the Archean Sparrow pluton, Slave Province, Canada

KEITH BENN*, NATALIE M. HAM and GEOFFREY S. PIGNOTTA

Ottawa-Carleton Geoscience Centre and Department of Geology, University of Ottawa, Ottawa, Canada ON K1N 6N5

and

WOUTER BLEEKER

Geological Survey of Canada, Continental Geoscience Division, 601 Booth Street, Ottawa, Canada ON K1A 0E8

(*Received* 23 *July* 1997; *accepted in revised form* 20 *April* 1998)

Abstract—The Sparrow pluton is part of the Prosperous Suite of two-mica granites that crop out within amphibolite grade meta-greywackes of the southern Yellowknife Domain, in the Slave Province of the Canadian Shield. The magnetic susceptibility (K) and the anisotropy of magnetic susceptibility (AMS) were used to systematically map the structural patterns in the pluton and to establish the relationship between plutonism and Late Archean tectonics in the region. Paramagnetic Fe-phyllosilicates (biotite, chlorite) and very fine-grained magnetite contribute to K and to the AMS. The magnetic foliation and the magnetic lineation are predominantly controlled by the biotite fabrics and their orientations are consistent with the regional D_2 strain field. The horizontal magnetic lineations in the Sparrow pluton suggest a horizontal stretching component associated with the regional D_2 event. The zonation defined by K values is compatible with a fold pattern trending parallel to the regional F_2 folds and S_2 foliation and to the magnetic fabric trends in the pluton. The intensities and symmetries of the AMS also define map patterns that are consistent with D_2 deformation. Microstructural study indicates the pluton recorded D_2 strain as it crystallized and cooled from the solidus, demonstrating syn-D_2 emplacement. The results indicate the pervasive structural patterns in the Sparrow pluton are an integral part of the regional strain field, and that they are kinematically consistent with a transpressive D_2 strain regime. Mapping the fabric patterns within syntectonic plutons provides a useful approach to the kinematic analysis of synemplacement deformation events in multiply deformed metamorphic terranes.

INTRODUCTION

The Prosperous Suite of granites is a regionally extensive plutonic assemblage that crops out within cordierite and andalusite-bearing metasedimentary rocks of the Yellowknife Domain in the Archean Slave Province of the Canadian Shield (Fig. 1; Henderson, 1985). The Prosperous Suite is a key element in the regional tectono-magmatic evolution because the plutons represent collisional-type granite magmatism associated with one of the main Late Archean tectonic episodes (Bleeker and Beaumont-Smith, 1995; Bleeker *et al.*, 1997a). Structural and magnetic fabric analyses of Prosperous Suite granites were undertaken as part of a wide-ranging study of the relationships between plutonism and tectonics in the Yellowknife Domain, in conjunction with a SNORCLE Lithoprobe deep-seismic transect that crosses the region (Fig. 1) and with the Slave Province NATMAP program. In this paper, we present a detailed investigation of the Sparrow pluton, one of the principal intrusions of the Prosperous Suite.

The work focused mainly on mapping the pervasive fabrics developed in the pluton during the magmatic and high-temperature subsolidus deformation that accompanied and followed emplacement. The fabrics were systematically mapped on a tight sampling grid (68 sites distributed over the 120 km^2 map area) using the low-field anisotropy of magnetic susceptibility (AMS) technique (Borradaile, 1988; Rochette *et al.*, 1992). Comparison with field measurements suggests the magnetic fabrics are predominantly controlled by the preferred orientations of paramagnetic biotite crystals, although paramagnetic chlorite and very fine-grained magnetite also contribute to the magnetic susceptibility and to the AMS. The magnetic fabric orientations are homogeneous at the outcrop scale and at the pluton scale, and define a pattern that is consistent with the regional D_2 strain field. The magnetic susceptibility, the degree of magnetic anisotropy and the shapes of the AMS ellipsoids also define patterns that can be related to D_2 deformation.

The results are of interest from both regional tectonic and thematic standpoints. Syntectonic emplacement of the pluton during the main phase of D_2 is demonstrated, hence new isotopic dates for the pluton

*E-mail: kbenn@uottawa.ca

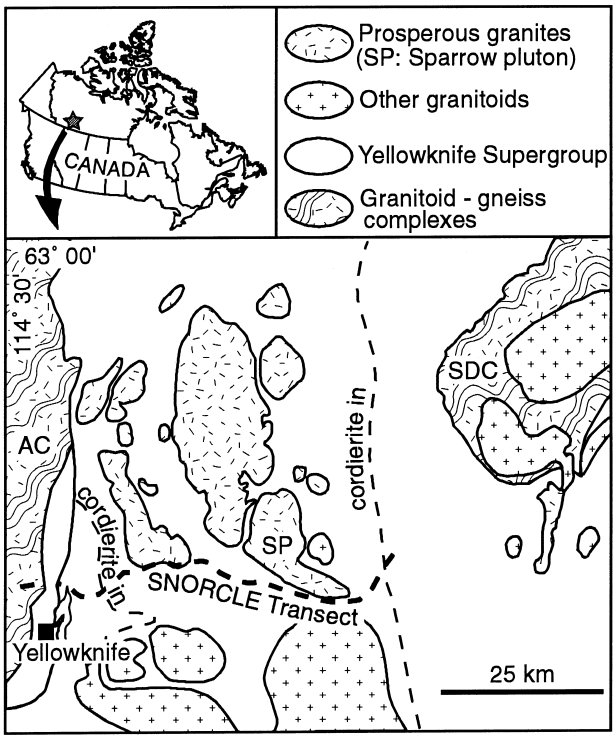

Fig. 1. Location and geology of the Yellowknife Domain, Slave Province. The trace of the SNORCLE Lithoprobe seismic transect is indicated by the heavy dashed line. SP: Sparrow pluton, SDC: Sleepy Dragon Complex, AC: Anton Complex.

(*ca* 2596 Ma) may be used to establish the age of this Archean tectonic event in the southern Slave Province. The fabrics documented using the AMS are compatible with transpressional synemplacement tectonics, indicating a horizontal Z-axis and an important component of horizontal stretching associated with the bulk regional D_2 strain. The horizontal stretching is inferred from the magnetic lineations in the pluton. The results demonstrate that in regions with complex deformation histories the internal fabrics of granite plutons can preserve a record of the strain field and kinematics associated with the synemplacement tectonic event.

TECTONIC AND STRUCTURAL SETTING

The Archean supracrustal rocks in the Yellowknife Domain (Fig. 1) belong to the Yellowknife Supergroup (Henderson, 1981, 1985) which is composed of mafic and felsic volcanic rocks at its base overlain by metasedimentary rocks of the Burwash Formation. The latter consists predominantly of turbiditic greywackes. The Sleepy Dragon Complex, a polyphase granitoid–gneiss complex that structurally underlies the Yellowknife Supergoup (Kusky, 1990; Bleeker *et al.*, 1997b) crops out in the eastern part of the region (Fig. 1).

Henderson (1981, 1985) interpreted the contact between the Sleepy Dragon Complex and the Yellowknife Supergroup as an unconformity, and proposed a tectonic model wherein the Yellowknife Supergroup represents the fill of an ensialic rift basin, bordered to the east by the Sleepy Dragon Complex and to the west by the Anton Complex (Fig. 1). Subsequent workers proposed that the Yellowknife Supergroup represents the remnants of an oceanic basin (Fyson and Helmstaedt, 1988) or a collage of arc assemblages, obducted oceanic crust and foredeep basin material (Kusky, 1989, 1990) thrust over the Sleepy Dragon Complex during a collisional event. In these models, calc-alkaline plutons such as the Defeat Suite granitoids (Fig. 2a) would represent subduction-related magmatism. Extensional faulting along the contact between the Yellowknife Supergroup and the gneisses of the Sleepy Dragon Complex may indicate late stage tectonic exhumation of the gneisses during crustal extension that followed thickening due to collision (James and Mortensen, 1992).

Three generations of structures are recognized by regional mapping of the Burwash Formation turbidites (Bleeker and Beaumont-Smith, 1995). The oldest regional foliation (S_1), a slaty cleavage, is axial planar to tight or isoclinal, upright, doubly-plunging folds (F_1, Fig. 2a). D_2 deformation caused regional-scale refolding (F_2), about mostly steeply plunging axes, of the F_1 fold belt and resulted in the development of the principal regional foliation, S_2, a NW- to N-trending crenulation cleavage. D_2 is interpreted to be the expression of regional dextral transpressive tectonics that was the far-field effect of a collisional event along the periphery of the proto-Slave craton as it existed *ca* 2600 Ma (Bleeker *et al.*, 1997a). The dextral transpressive nature of D_2 deformation is inferred from the kinematics of discrete late-D_2 strike-slip shear zones and from the pattern of refolding of F_1 folds. The D_2 event resulted in fold interference that produced steeply plunging mushroom folds (Fig. 2a & b) in the supracrustal cover and in the structurally lower basement complexes (Bleeker, 1996). Regionally developed extension lineations associated with the main D_2 deformation phase are notably lacking in the Yellowknife Domain. Late during the D_2 event, deformation was localized within discrete shear zones, such as the Watta Lake and Yellowknife River Deformation Zones (Fig. 2a), which contain shallowly plunging extension lineations and associated dextral shear sense indicators (Bleeker and Beaumont-Smith, 1995). Locally, younger NE-trending F_3 folds and an associated coarsely spaced crenulation cleavage (S_3) overprint D_1 and D_2 structures. Retrograde chlorite is associated with S_3.

The Prosperous Suite plutons outcrop within the Burwash Formation along a broad N–S-trending culmination of andalusite–cordierite facies metamorphism, outlined by the cordierite-in isograds (Fig. 1). The Prosperous Suite is composed of predominantly homogeneous, medium-grained muscovite–biotite granites with associated pegmatitic phases. The granites contain

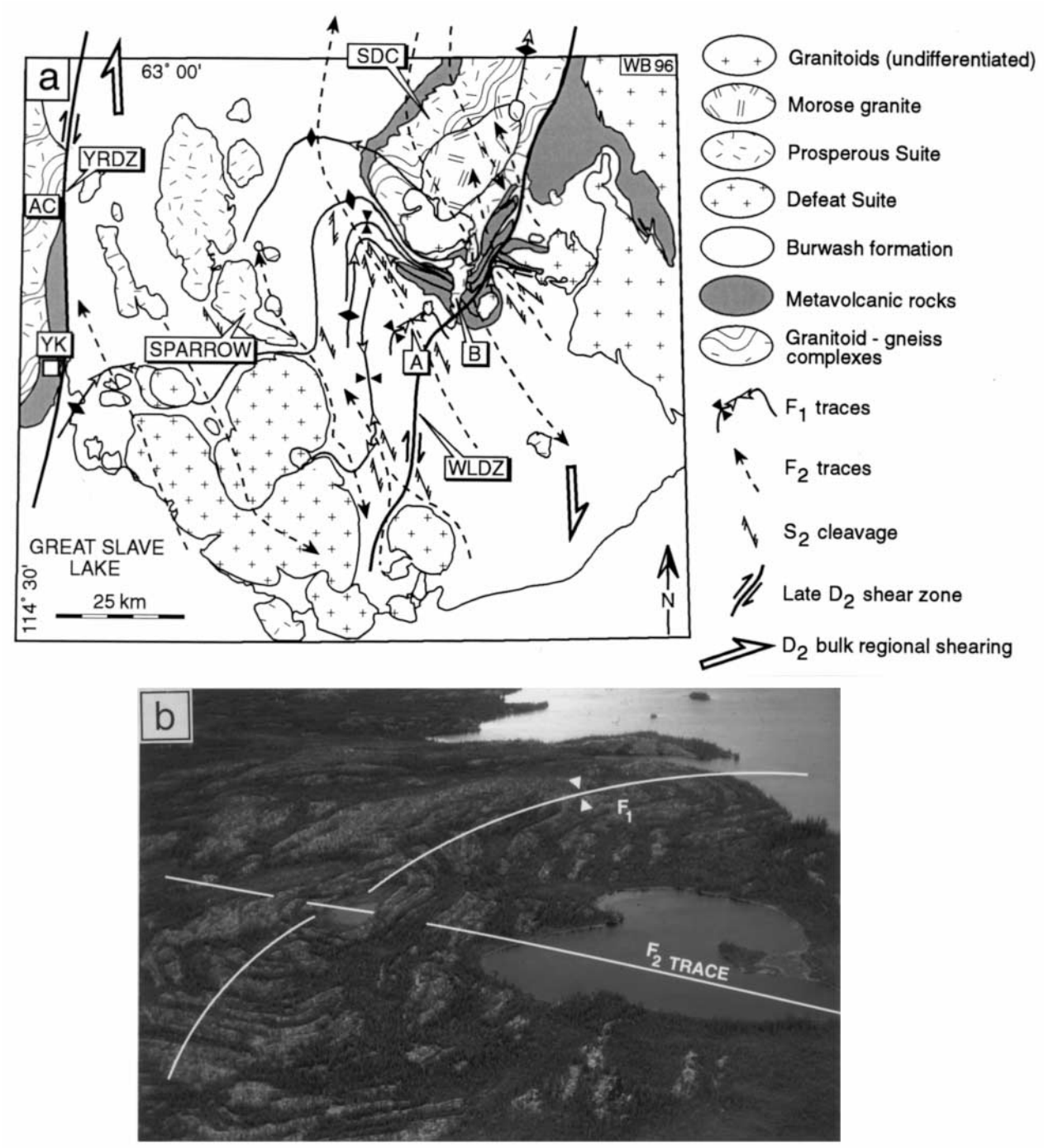

Fig. 2. (a) Synoptic map of the Yellowknife Domain with the principle geology and structures, showing the Prosperous Suite (Sparrow pluton indicated) in the context of F_1 and F_2 folds and the overall D_2 deformation field. WLDZ: Watta Lake Deformation Zone; YRDZ: Yellowknife River Deformation Zone; A: location of (b); B: an intrusion of the Prosperous Suite cross-cuts an F_1 fold axial surface trace; SDC: Sleepy Dragon granitoid–gneiss complex; AC: Anton granitoid–gneiss complex; YK: town of Yellowknife. (b) Aerial photograph of an F_1–F_2 mushroom interference structure at locality A in (a).

plagioclase of composition An_5 and are locally tourmaline bearing (Kretz *et al.*, 1989). The contact metamorphic assemblage of cordierite + andalusite indicates pluton emplacement at depths corresponding to between 200 and 400 MPa (Kretz *et al.*, 1989). Based on their characteristic mineralogy, the Prosperous Suite plutons are peraluminous (Clarke, 1981) and can be tectonically classified as the C_{ST} granite type (''Crustal Shearing and Thrusting'', Barbarin, 1990) implying intra-crustal magma genesis during a collisional event. The granites and pegmatites also form abundant dykes and stocks that crop out between the main plutons. Some dykes contain andalusite consistent with emplacement at pressures of less

than 400 MPa. Emplacement of the Prosperous granites post-dated D_1 since one of the intrusions cross-cuts a regional F_1 fold (B in Fig. 2a). Structures and microstructures within the Sparrow pluton can be used to infer syn-D_2 emplacement.

STRUCTURES AND MICROSTRUCTURES

A penetrative, homogeneous mesoscopic-scale foliation is distinguished in many granite outcrops. The foliation is defined by mostly euhedral, apparently igneous biotite and plagioclase crystals suggesting that fabric formation began during deformation of the crystallizing magma (Paterson *et al.*, 1989; Bouchez *et al.*, 1990). A minor but penetrative high-temperature subsolidus deformation of the pluton is indicated by the dynamic recrystallization of quartz (assumed to be the last mineral to crystallize from the magma) into aggregates of new grains (Fig. 3a), suggesting that the foliation records a continuum in deformation from the magmatic state to high-temperature subsolidus conditions. In the northern, roughly rectangular region of the pluton the evidence of subsolidus deformation is restricted to subgrain development and minor recrystallization of quartz. In the southern 'tail' of the pluton the quartz is largely recrystallized, especially near the pluton margins, and the homogeneous foliation is more strongly expressed than in the northern region.

Field measurements of the foliation indicate predominantly NNW- to NW-strikes parallel to the regional S_2 foliation trajectories, and moderate to steep dips, implying continuity in the D_2 strain field recorded by the magmatic to high-temperature subsolidus foliation in the granites and by the structures in the surrounding country rocks (Paterson and Tobisch, 1988). This interpretation is further supported by the magnetic data that provide a much more complete fabric picture (see below). The knife-sharp margin of the pluton is exposed at the southeastern tip of the pluton's tail. There, the contact is perpendicular to the S_2 foliation in the host rocks *and* to the homogeneous foliation in the granites. This outcrop-scale observation emphasizes that the discordant nature of the Sparrow–country rock contact (along the northern and southern borders of the pluton) with respect to the S_2 foliation is in no way an indicator of post-D_2 emplacement.

Further D_2 deformation of the granites was concentrated into decimetre- to metre-scale protomylonitic strike-slip shear zones (Fig. 3b) that likely formed once the rocks had cooled to temperatures below 550°C (Gapais, 1989). Northwest- to N-striking shear zones are dextral, consistent with bulk regional dextral D_2 shearing. A second family of predominantly NW- to E–W-striking shear zones is sinistral and kinematically consistent with the apparent sinistral deflection of the southern tail of the pluton where this family of shear zones was observed. Localized sinistral shearing was likely induced by the presence of an older, rigid pluton of the Defeat Suite located just to the south (Fig. 2a). Granitic and pegmatitic dykes of the Prosperous Suite observed near the Sparrow pluton are folded with axial surfaces parallel to S_2 (Fig. 3c) further suggesting D_2 deformation during granitic magmatism.

AMS METHOD

Sixty-eight sampling sites were established within the 120 km^2 map area of the Sparrow pluton. Distances between sites are less than 2 km, and in many cases less than 1 km. Two 25 mm diameter oriented drill cores were collected at each site, and two 22 mm long cylindrical specimens were cut from each of the cores. The use of four specimens per site (43 cm^3 of rock) and a 1–2 km sampling grid should provide sufficient sampling to characterize the AMS in homogeneous granites of medium grain size (Olivier *et al.*, 1997). The AMS was measured on a Kappabridge KLY-2 instrument at the University of Ottawa. Treatment and statistical analyses of the data followed the procedures described in Benn *et al.* (1997) and the full AMS data set is available from the first author.

Two standard scalar parameters were used to describe the degree of anisotropy and shapes of the AMS ellipsoids (Tarling and Hrouda, 1993). The degree of anisotropy is expressed as

$$P'\% = (P' - 1) \times 100, \tag{1}$$

where

$$P' = \exp\sqrt{\left\{2\left[(\eta_1 - \eta_m)^2 + (\eta_2 - \eta_m)^2 + (\eta_3 - \eta_m)^2\right]\right\}}, \tag{2}$$

$\eta_i = 1\mathrm{n}(K_i)$ (i = 1–3) and $\sqrt[3]{\eta_1 \cdot \eta_2 \cdot \eta_3}$. The shape of the ellipsoid is described by

$$T = 2\left(\frac{\ln K_2 - \ln K_3}{\ln K_1 - \ln K_3}\right) - 1, \tag{3}$$

where $T = 1$ and $T = -1$ indicate, respectively, perfectly oblate and perfectly prolate ellipsoids. We chose to calculate $P'\%$ and T after correction of K_i by addition of an isotropic diamagnetic component ($K_{\mathrm{dia}} = -6 \times 10^{-6}$ SI) carried by all minerals (Rochette, 1994), but which is dominated by quartz and feldpar because these diamagnetic minerals represent >85% of the rock. The correction is applied for rocks with very low susceptibilities in order to give $P'\%$ values that more closely reflect the anisotropies due to the paramagnetic and ferromagnetic components of the AMS.

Many previous studies have shown that the principal axes of the AMS are often parallel to the principal penetrative structural anisotropies in rocks.

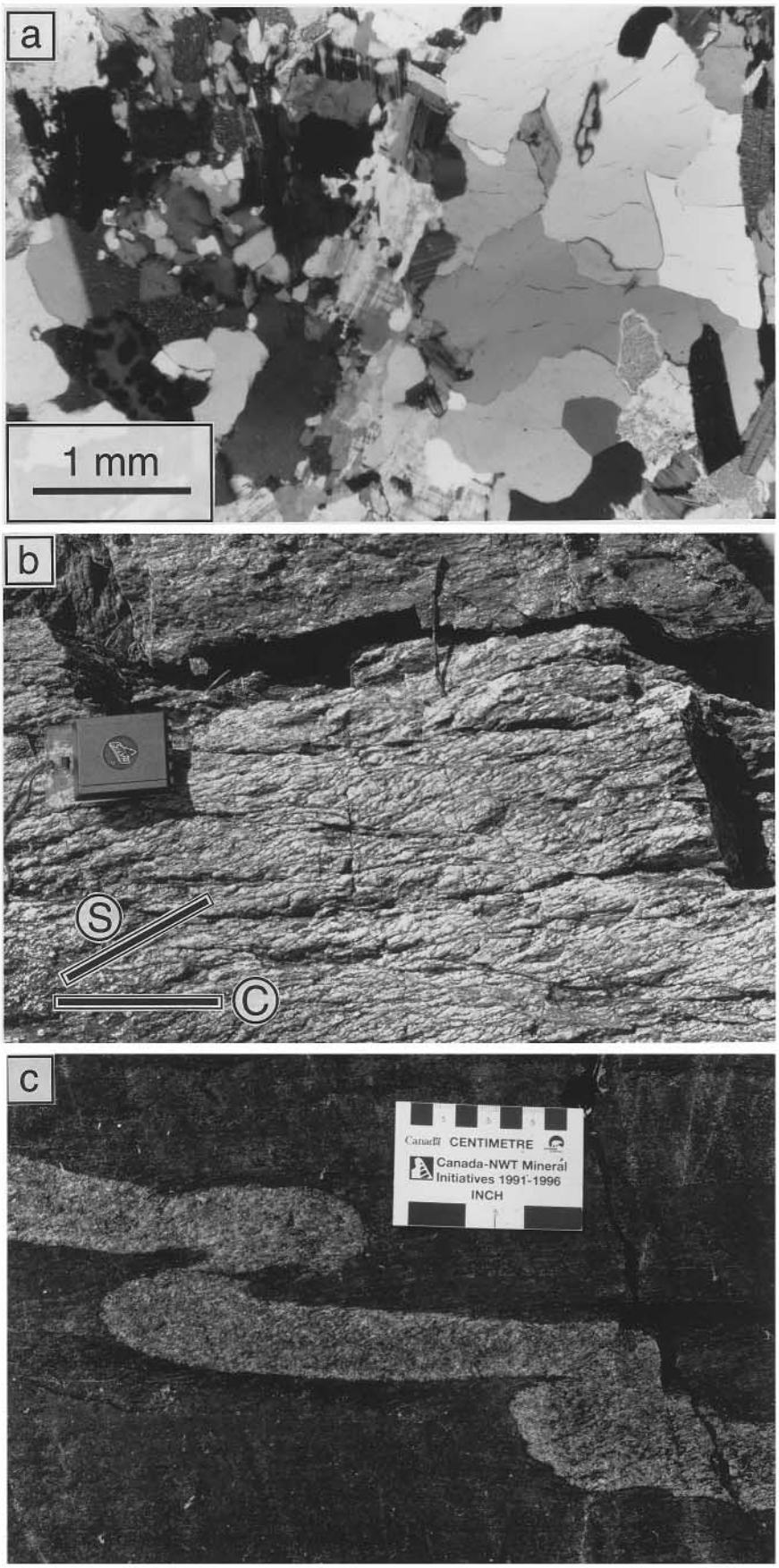

Fig. 3. (a) Photomicrograph showing large subgrains of quartz with straight extinction in the right half of the figure. (b) A small-scale discrete shear zone in the Sparrow pluton, with a Silva compass for scale. (c) A folded dyke of Prosperous granite with S_2 axial-planar cleavage, located a few hundred metres east of the Sparrow pluton within the Burwash Formation. The long dimension of the photograph is roughly N–S.

Commonly, the measured K_3 axis (the pole to the *magnetic foliation*) is perpendicular to a structural foliation whereas the K_1 principal direction (the *magnetic lineation*) is parallel to a structural lineation. The presence of more than one foliation in a rock may give rise to composite magnetic fabrics not simply related to the petrofabric (Housen *et al.*, 1993; Aranguren *et al.*, 1996; Riller *et al.*, 1996); we have observed no mesoscopic or microscopic evidence of multiple mineral fabrics in our samples. Anomalous magnetic fabrics can also arise due to the presence of minerals with inverse intrinsic magnetic anisotropies (Rochette *et al.*, 1992). Therefore, interpretation of the AMS requires investigation of the minerals that contribute to the induced magnetization.

Study of thin sections revealed the presence of biotite, and also chlorite that has locally replaced biotite. Both of these iron-rich paramagnetic minerals contribute to the magnetic fabric. Tourmaline is also present locally in the pluton, forming polycrystalline clusters a few centimetres in diameter. Care was taken not to collect tourmaline-bearing samples since this mineral has an inverse intrinsic AMS. Petrographic study also indicates that coarse-grained opaque minerals, e.g. primary magnetite, are absent from our samples. Small amounts of fine-grained ferromagnetic crystals, difficult to identify by standard optical microscopy, may contribute significantly to the susceptibility and its anisotropy. This may be especially true for rocks with very low bulk susceptibilities like the Sparrow granites (Fig. 4a). A study of the hysteresis properties and the coercivities of the granites was carried out to determine the relative contributions to the bulk susceptibilities (K) from the paramagnetic component (K_{para}, attributed to biotite and chlorite) and from the ferromagnetic component (K_{ferro}), and to identify the ferromagnetic mineralogy.

An alternating gradient force magnetometer (Micromag) at Lakehead University was used to establish hysteresis loops for granite fragments weighing between 10 and 20 mg. Measurements were made on eight fragments, four from each of two specimens which had been used in the low-field AMS study. All the fragments contained both mafic and felsic minerals. Fields up to 500 mT were used in order to saturate the ferromagnetic minerals. The value of K_{para} was deduced from the slope of the linear part of the hysteresis loops where the ferromagnetic minerals were saturated. Removing the slope of the linear part of the hysteresis loops allows determination of K_{ferro} (Borradaile and Werner, 1994). Results show that all of the studied fragments had ferromagnetic contributions greater than 20% of their paramagnetic susceptibilities (Fig. 4b).

Coercivities (H_c), saturation remanence (M_r) and saturation magnetization (M_s) were obtained from the hysteresis loops, and coercivities of remanence (H_{cr}) were determined through demagnetization of saturation remanence using the Micromag. The H_c values (between 17.2 and 72.2 mT) and the H_{cr} values (between 34.1 and 71.1 mT) are comparable to pub-

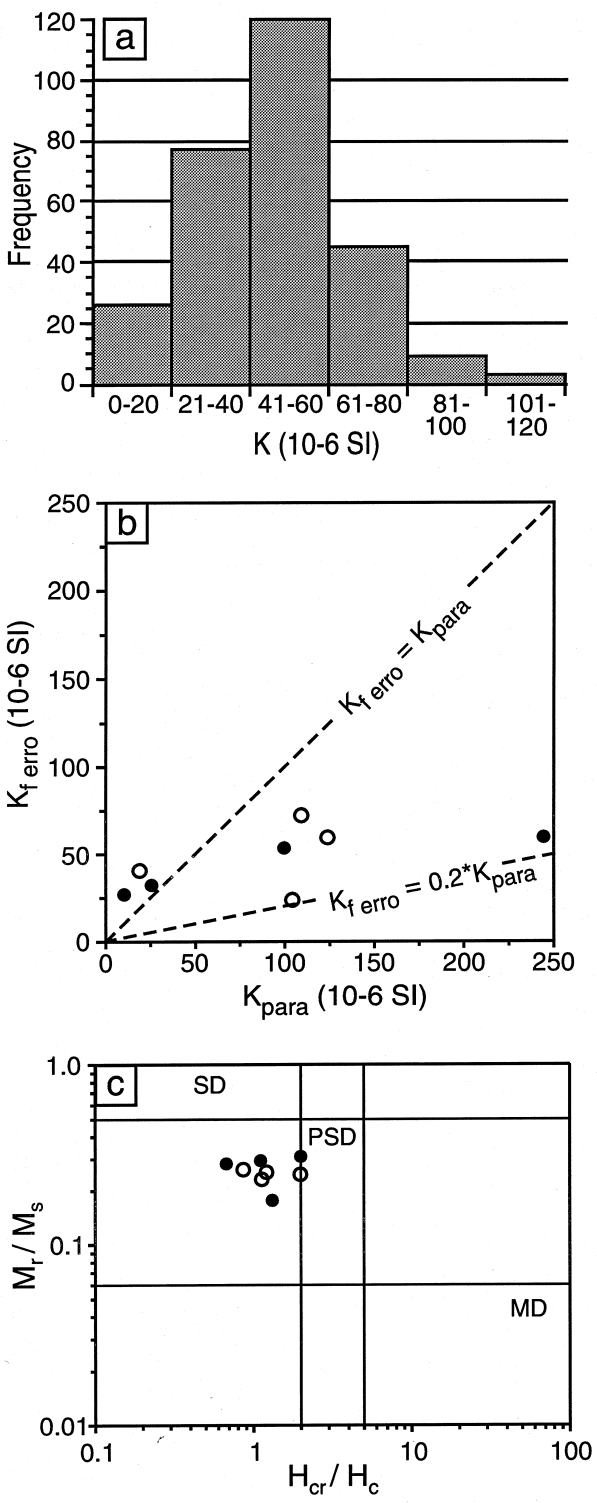

Fig. 4. (a) Histogram of the average susceptibilities (K) for all specimens. (b) Plot of the paramagnetic (K_{para}) and ferromagnetic (K_{ferro}) contributions to the magnetic susceptibilities. (c) Domain structures of magnetite based on the ratio of saturation remanence (M_r) to saturation magnetization (M_s) and on the ratio of coercivity of remanence (H_{cr}) to coercivity (H_c). SD: single domain; PSD: pseudo-single domain; MD: multi domain. Diagram modified after Day *et al.* (1977) and Borradaile and Werner (1994). In (b) and (c), black dots are for sample 96SP60 and open circles are for sample 96SP49.

lished coercivities for very fine-grained magnetite (Heider *et al*., 1987, 1996) suggesting this mineral is the predominant carrier of the K_{ferro} component in our samples. Remanence and coercivity ratios are plotted in Fig. 4(c), which is a diagram modified from Day *et al*. (1977) with boundaries taken from Borradaile and Werner (1994). The plot suggests the presence of very fine-grained magnetite, possibly with pseudosingle-domain behaviour. Comparison of the data in Fig. 4(c) with data in figs 7.10 and 7.11 of O'Reilly (1984) indicates magnetite grain sizes on the order of 1–10 μm.

AMS RESULTS

Foliation and lineation

The directional components of the AMS are plotted on maps in Figs 5(a) and 6. Field measurements of the mesoscopic foliation in the pluton are plotted in Fig. 5(b) for comparison with the magnetic foliation. The orientation data for magnetic fabrics and field measurements are also plotted on lower-hemisphere Schmidt projections in Fig. 7, where the data are shown separately for the northern region and the southern tail region of the pluton. Inspection of Figs 5–7 immediately reveals that the magnetic fabric orientations define very consistent patterns in both the northern and southern regions that can be directly compared to the orientations of the mesoscopic foliation measured in the granites and to the orientations of the D_2 structures in the country rocks.

In the northern region, the magnetic foliation strikes NNW–SSE and has variable but mostly steep dips (Figs 5a & 7a). In the southern region, the magnetic foliation is rotated in a counter-clockwise sense with respect to the fabrics in the northern region, striking NW–SE and dipping steeply at most outcrops (Figs 5a & 7d). The counter-clockwise rotation of the magnetic foliation in the southern region is coincident with the apparent sinistral deflection of the pluton's tail.

Comparison of the maps in Fig. 5 and the Schmidt projections in Fig. 7(a, b, d & e) reveals that the magnetic foliation and the mesoscopic (biotite) foliation have similar strikes at almost all the sampled outcrops, and this argues for a strong control of the biotite preferred orientation on the magnetic fabric. The dips of the magnetic and mesoscopic foliations differ significantly at some outcrops, and in a few cases shallowly dipping NE–SW-striking magnetic foliations were measured at sites where field measurements indicate a more steeply dipping NW–SE-striking mesoscale foliation (compare Fig. 5a & b). The more variable dips displayed by the magnetic foliations may result from the influence of fine-grained magnetite crystals on the bulk AMS, causing the orientation of the magnetic fabric to deviate from the mesoscopic foliation. Alternatively, at some sampling sites the magnetic fabrics may provide a more precise determination of the fabric orientation than the field measurements.

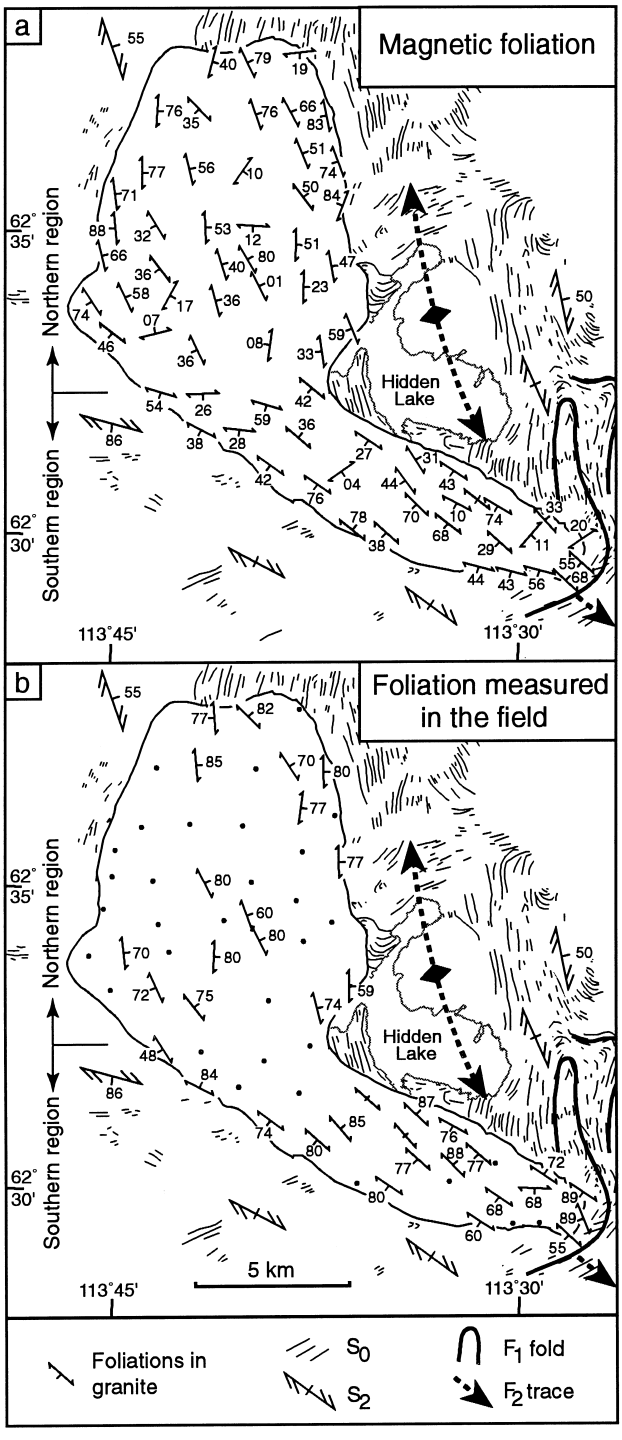

Fig. 5. Maps of (a) the magnetic foliation and (b) the mesoscopic-scale foliation in the Sparrow pluton. Sampling sites are located at the middle of the foliation symbols. In (b), dots indicate magnetic fabric stations where no field measurements of the foliation could be made. Bedding (S_0) traces and foliation (S_2) in the country rocks are taken from Henderson (1985).

In both the northern and the southern regions, the magnetic lineations have strong NNW–SSE- to NW–SE-trending and shallowly plunging preferred orientations. Since mesoscopic linear fabrics are not present in the granites it is not possible to make a direct com-

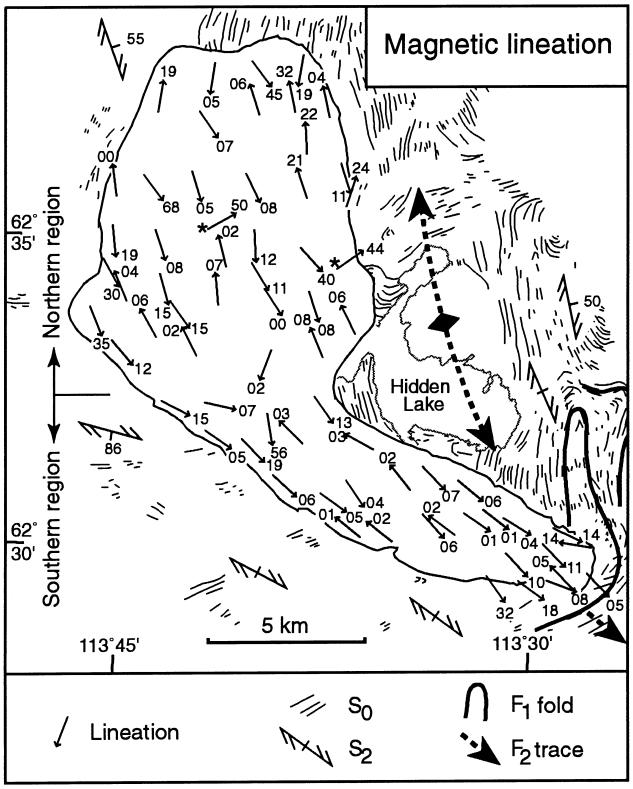

Fig. 6. Map of the magnetic lineations in the Sparrow pluton. Sampling sites are located at the tails of the lineation symbols. Asterisks indicate probable anomalous magnetic lineations (see text). Bedding (S_0) traces and foliation (S_2) in the country rocks are taken from Henderson (1985).

parison between the magnetic lineations and field measurements. In light of the influence of the biotite foliation on the magnetic fabric, the strongly oriented magnetic lineation is interpreted to be predominantly controlled by the biotite fabric at most sampling sites. Neither the presence of fine-grained magnetite nor the local replacement of biotite by chlorite seem to have a strong effect on the lineation orientations which are quite consistent (Figs 6, 7c & f). Major contributions to the AMS from pseudosingle-domain magnetite crystals would most probably cause increased scatter in the lineation orientations and possibly flipping of the magnetic fabric axes (Rochette *et al*., 1992), like at the two stations indicated by asterisks in Fig. 6 where NE-trending magnetic lineations were measured. Owing to the highly oblate shape of the intrinsic AMS ellipsoids of biotite crystals, with the K_3 principal direction lying close to the crystallographic *c*-axis and very little magnetic anisotropy in the basal plane (Borradaile and Werner, 1994), the strongly oriented magnetic lineation is parallel to the zonal axis about which the biotite basal planes are aligned (Bouchez, 1997).

Average susceptibilities

In granite massifs where K is dominated by contributions from paramagnetic minerals, the magnetic susceptibility can be used as a petrological mapping tool because K values are a linear function of the iron content in the paramagnetic minerals (Gleizes *et al*., 1993). A simple correlation between the spatial distribution of K values and petrological zonations cannot be made with certainty for the Sparrow pluton because of the ferromagnetic contribution to the susceptibilites (Fig. 4b). However, the mapping of K values on a tight sampling grid in the Sparrow pluton reveals a distinct pattern that is useful from a structural standpoint since it can be related to the regional strain field.

A contoured map of the site average magnetic susceptibilities is presented in Fig. 8(a). The overall variations are small ($22 \leq K \leq 98$) but a zonation pattern is recognized that suggests the presence of NNW- to NW-trending folds. This is most evident in the northern region, where the broad zone defined by $50 < K < 75$ crosses the entire pluton and is highly discordant to the magnetic fabrics, defining an apparently doubly-plunging fold pattern. This interpretation is supported by the fact that the fold trends are parallel to the average foliation strikes and to the magnetic lineation in the pluton, and to the regional D_2 structural trends in the host rocks. The interpretation implies that the K values in the northern part of the pluton define a thin and horizontal zonation that is parallel to the map section and to the bulk shortening recorded by the foliation. In the southern region, several narrower zones are discordant to the magnetic fabric trajectories and may be folded with an axial surface trace that is parallel to the NW-trending magnetic fabrics.

Anisotropies and shapes of the AMS ellipsoids

Contoured maps of the degree of anisotropy ($P'\%$) and the ellipsoid shapes (T) are shown in Fig. 8(b & c). $P'\%$ values are generally higher in the southern tail of the pluton coinciding with the more strongly expressed mesoscopic foliation in that region. The contoured area corresponding to $P'\% > 6$ extends into the northern region of the pluton where it defines two NW–SE elongate lobes oriented parallel to the magnetic fabric trends. The map of T values shows elongate NW–SE-trending corridors defined by more oblate ($T > 0$) and more prolate ($T < 0$) AMS. The horseshoe-shaped zone of oblate fabrics in the northern region closes at a site where $T = 0.08$, i.e. where the AMS has a nearly neutral shape, and so the two limbs of the horseshoe may be considered as two separate corridors. The corridors defined by oblate and prolate fabrics are parallel to the trends defined by the magnetic fabrics.

DISCUSSION

The Sparrow pluton is characterized by penetrative fabric anisotropies that were systematically mapped

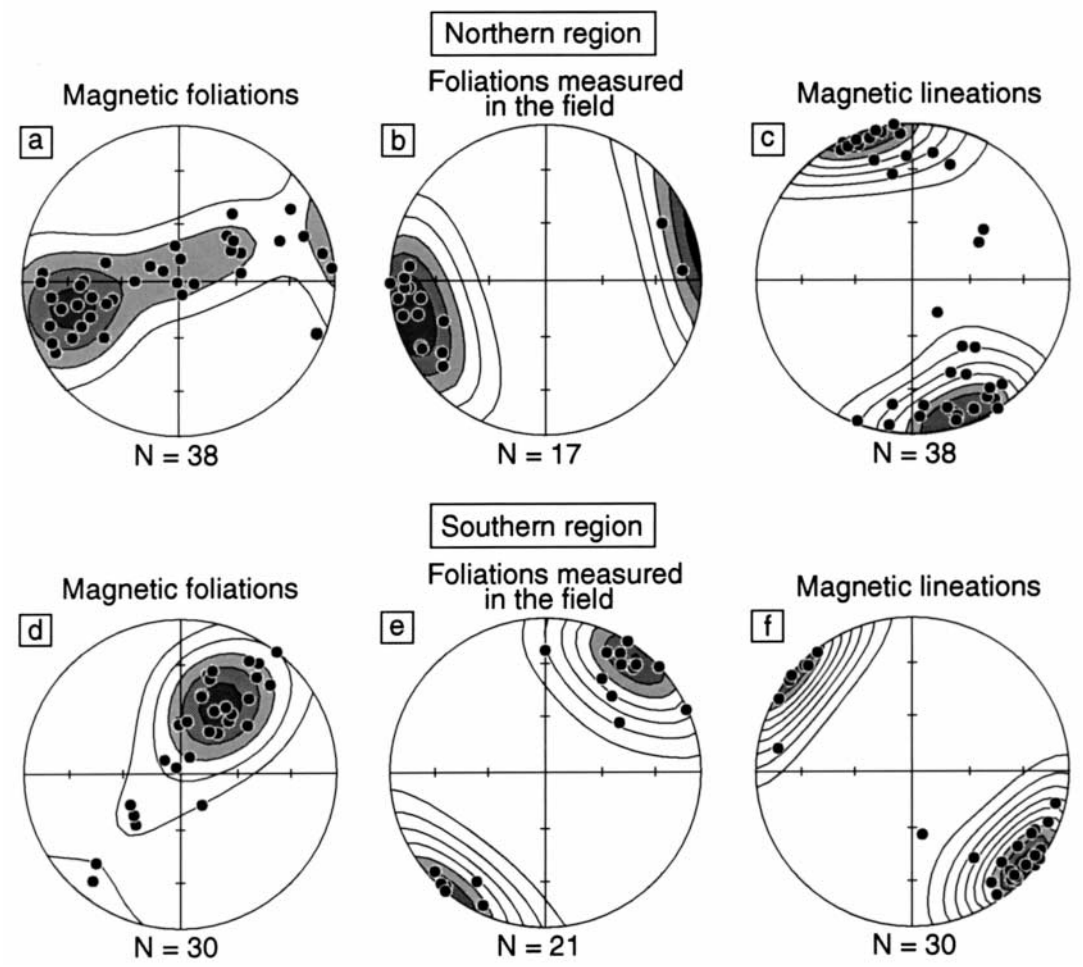

Fig. 7. Lower-hemisphere Schmidt projections of (a & d) the magnetic foliation poles, (b & e) the poles to the mesoscopic-scale foliation measured in the field and (c & f) the magnetic lineations for the northern and southern regions of the Sparrow pluton. Contour intervals are at 3σ.

using the directional and scalar parameters of the anisotropy of magnetic susceptibility. With the exception of some field measurements of the mesoscopic foliation (Fig. 5b) none of the structural information provided by the magnetic study could be obtained by conventional mapping methods. Microstructures suggest that formation of the penetrative fabrics began during crystallization of the granitic magma and continued during the early stages of subsolidus cooling of the pluton. The structural picture provided by the magnetic data can be used to confirm syn-D_2 emplacement of the Sparrow pluton and to shed new light on the kinematics of the D_2 event that was concurrent with granitic magmatism in the Yellowknife Domain.

The AMS signature and syn-D_2 emplacement

The structural patterns revealed by the magnetic data are signatures of the regional D_2 structural event. This is shown by direct comparison of the maps of magnetic data with the D_2 structures in the surrounding Burwash Formation. Since the penetrative structures in the pluton record deformation of the crystallizing magma and the still hot granites as they cooled from the solidus, the magnetic data demonstrate syn-D_2 emplacement.

1. Despite the contributions to the AMS from multiple mineral sources, the magnetic foliation orientations are comparable to the mesoscopic foliation that is defined by the preferred orientations of biotite crystals. The systematic mapping of the magnetic foliation confirms the field observations of a penetrative NNW-striking (in the northern region) to NW-striking (in the southern region), predominantly steeply dipping-foliation in the pluton. The foliation is parallel to the axial surface traces of F_2 folds in the country rocks and is consistent with regional horizontal D_2 shortening.
2. The well-defined magnetic lineation is interpreted to be parallel to the biotite lineation at most sampling sites, i.e. the K_1 principal direction of the AMS is parallel to the zone axis about which the biotite basal planes are aligned (Bouchez, 1997). The magnetic (biotite) lineation is considered to indicate the maximum principal stretch recorded during the late stages of crystallization and the early stages of cooling of the fully crystallized granite. This interpret-

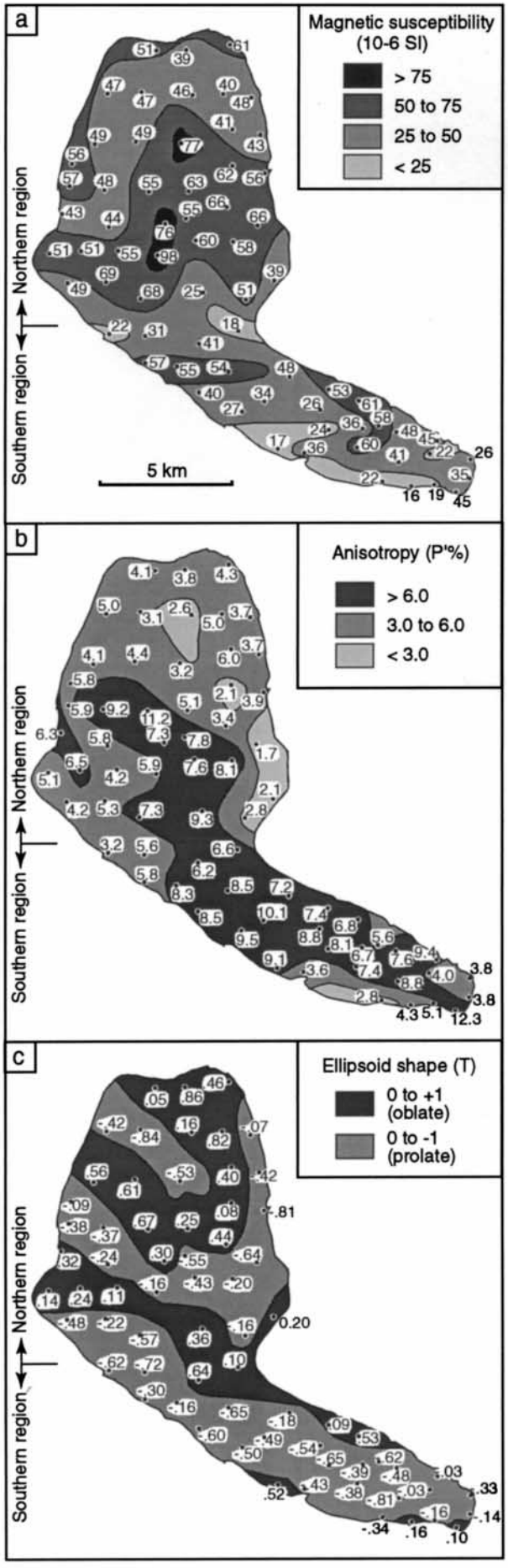

ation is based on the results of numerical models of fabric development (Blanchard *et al.*, 1979) showing that during progressive deformation, dilute suspensions of rigid platy crystals with initially random orientations adopt a zonal arrangement about an axis close to the maximum principal stretch. This is expected to occur in a deforming magma of low crystal fraction. Any inherited weak preferred orientation of the platy crystals might be overprinted after about 10–15% of superimposed strain, so that the lineation would be close to the *X*-axis of the superimposed strain (Benn, 1994). The fabric orientation tends to become steady state due to the increasing physical interactions between crystals at advanced stages of crystallization and at higher strains, and due to the averaging effects of subfabrics corresponding to crystals with different shapes (Tikoff and Teyssier, 1994; Arbaret *et al.*, 1997; Bouchez and Benn, 1997; Ildefonse *et al.*, 1997). The mapped magnetic lineation is interpreted to indicate a strong component of NNW to NW horizontal stretching associated with D_2 deformation of the crystallizing and cooling Sparrow pluton.

3. The zonation defined by the *K* values shows an apparent NNW- to NW-trending fold pattern (Fig. 8a) parallel to the fabric trends in the pluton and to the trends of F_2 folds in the Burwash Formation. Hence the fold pattern in the pluton is interpreted to have formed in response to the same regional D_2 horizontal shortening that is recorded by the magnetic foliation and the magnetic lineation, and that affected the pluton as it crystallized and cooled. This interpretation implies that the mapped zonation formed in the crystallizing magma or within the still hot and ductile pluton. It may be that the magnetic susceptiblity zonation outlines a petrological layering formed by injection of multiple sills and/or by fractional crystallization (see for example Mahood *et al.*, 1996). Alternatively, the zonation may indicate a late-magmatic alteration pattern, possibly related to the production of fine-grained magnetite. Whatever the petrological significance of the zonation may be, the corresponding map pattern defined by the magnetic susceptibility data provides a useful structural criterion for syn-D_2 pluton emplacement.
4. The patterns defined by P'% and *T* are also consistent with emplacement and deformation of the Sparrow pluton during D_2. Both of these parameters can be strongly affected by small variations in magnetite content (Borradaile and Henry, 1997). However, the generally higher anisotropy (P'%) values in the southern region of the pluton are coincident with the more strongly expressed foliation

Fig. 8. Contoured maps of (a) the average susceptibilities (*K*), (b) the degrees of anisotropy (P'%) and (c) the AMS ellipsoid shapes (*T*).

there as compared to most of the northern region, judging from field observations. This suggests that the mapped pattern of P'% values can be used as a rough indicator of the relative strengths of the preferred orientations of the fabric-defining magnetic minerals. In the northern region, higher P'% values are located mostly in the central part of the pluton. This might be explained if tectonic deformation and fabric development were concentrated within the core of the pluton that would have crystallized and cooled more slowly than the margins of the pluton. The orientations of the NNW- to NW-trending elongate corridors defined by T values are similar to the patterns defined by other directional and scalar parameters of the AMS, suggesting the spatial distribution of AMS ellipsoid shapes is also consistent with D_2 deformation of the pluton.

Magnetic fabrics and regional kinematics

The dextral transpressive nature of D_2 tectonics in the Yellowknife Domain has been interpreted from the pattern of refolding of F_1 folds (Fig. 2a) and from the presence of discrete late-D_2 dextral shear zones (Fig. 2a; Bleeker and Beaumont-Smith, 1995), both of which suggest an important transcurrent component for the D_2 event. A more detailed kinematic analysis of D_2 deformation in the supracrustal rocks of the Yellowknife Supergroup is rendered difficult because the strain is superimposed on the older D_1 deformation including tight or isoclinal, upright, doubly-plunging F_1 folds (Fig. 2a & b). This has resulted in mostly steeply plunging F_2 folds and a somewhat complex total strain pattern. Locally, the strain pattern is further complicated by later F_3 folding and S_3 cleavage development. D_2 extension lineations are not widely developed in the Burwash Formation, so the directions of tectonic stretching associated with the main phase of this event have not been documented.

Jamison (1991) examined the kinematics of strain associated with compressional folding of initially horizontal layers and showed that a significant amount of fold axis-parallel extension is diagnostic of transpression. Jamison's (1991) model results are not directly applicable to kinematic analysis of the D_2 event in the Burwash Formation due to the complex total ($D_1 + D_2$) strain pattern, but the results may be more applicable to the deformation recorded within the Sparrow pluton that is revealed by the magnetic data. The pluton has been affected by one phase of pervasive strain (D_2) which produced the NNW- to NW-striking foliation, the NNW- to NW-trending horizontal lineation and the folding of a horizontal zonation revealed by the map of K values. The magnetic foliations indicate horizontal shortening and the magnetic lineations suggest an important stretch parallel to the axis of folding in the granites, as predicted in the models of Jamison (1991). Therefore, the magnetic fabric maps provide new corroborative evidence for the interpretation of D_2 as a transpressive tectonic event in the Yellowknife Domain.

Fabrics in plutons and terrane analysis

The results presented in this paper highlight the usefulness of fabric studies in granites for the analyses of multiply deformed metamorphic terranes. The internal fabrics of plutons can preserve a record of the regional deformation associated with the synmagmatic tectonic event, whereas the structural picture in the country rocks may be complicated by the superposition of different generations of structures. In the present case, the detailed magnetic fabric maps allowed the extraction of new information on the strain field and kinematics of a principal Late Archean tectonic episode in the southern Slave Province. The structural analysis of the Sparrow pluton has clearly shown that it was emplaced during the regional D_2 deformation, which may now be dated using geochronological data from the granites.

The tectonic fabric signatures of granites may be most strongly developed in plutons that, like the Sparrow, were emplaced within high-grade terranes such as the metasedimentary rocks of the Burwash Formation. In such a metamorphic environment crystallization and cooling will be relatively slow, and pervasive tectonic deformation of the pluton may occur as its viscosity gradually approaches the viscosity of the thermally softened host rocks (Pavlis, 1996). The Trois-Seigneurs pluton (Leblanc *et al.*, 1996) and the Rose Blanche granites (Benn *et al.*, 1993) are other examples of syntectonic granitoids emplaced within amphibolite-facies metasedimentary rocks, for which AMS data demonstrate a well-defined tectonic fabric. An implication is that mineral preferred orientations developed during magma emplacement might be overprinted by tectonic deformation late in the pluton crystallization history. Fowler and Paterson (1997) and Paterson and Miller (1998 this issue) provide field data suggesting magmatic fabrics formed late during emplacement of the Mount Stuart Batholith within the amphibolite-grade Chiwaukum Schist, since the fabrics formed after the incorporation of stoped blocks into the crystallizing magmas.

On the contrary, plutons emplaced within cold, rigid country rocks of low metamorphic grade would freeze more quickly and may undergo less penetrative tectonic strain than plutons emplaced within higher-grade crust, and in this case the fabrics may preserve the kinematics of magma flow into the growing pluton. The Lebel Stock (Cruden and Launeau, 1994) and the Dinkey Creek and Bald Mountain plutons (Tobisch and Cruden, 1995) represent examples where the AMS has been used to map apparently buoyancy-driven

magma flow patterns. Transitional cases may occur where fabrics related to emplacement flow or to the internal dynamics of magma chambers are only partly overprinted by synemplacement tectonics late during pluton crystallization. An example is the South Mountain Batholith where the preserved fabrics provide information on emplacement dynamics and on the synemplacement regional deformation event (Benn *et al*., 1997).

CONCLUSIONS

The magnetic susceptibility and the anisotropy of susceptibility (AMS) were used to derive detailed maps of the pervasive structural anisotropies that record magmatic to high-temperature subsolidus deformation of the Late Archean Sparrow granite pluton. The efficiency of the AMS technique for the structural mapping of granitoid plutons is strongly emphasized since little of the structural information inferred from the magnetic data could have been gathered using standard field methods. The mapped structural patterns in the pluton are directly comparable to the regional structures in the country rocks, and the strong tectonic signature of the magnetic fabrics confirms pluton emplacement during the main phase of regional D_2 tectonics in the Yellowknife Domain.

The magnetic data from the Sparrow pluton also provide new information on the kinematics of the D_2 event. The patterns defined by the magnetic foliation, the magnetic lineation and the bulk susceptibility suggest that deformation and folding of the pluton involved fold axis-parallel stretching, consistent with deformation of the crystallizing magmas and of the solidified but still hot granite in a transpressive tectonic regime. In the absence of widely developed extension lineations in the country rocks, the magnetic lineations in the Sparrow pluton represent the best available evidence for the horizontal stretching associated with D_2 transpression.

In regions with complex deformation histories the internal fabrics of granite plutons can preserve a record of the strain field and kinematics associated with the synmagmatic tectonic event. The magnetic fabrics in the Sparrow pluton provide a simpler and more easily derived picture of D_2 strain than can be obtained from the multiply deformed country rocks. The tectonic signatures of the fabrics in syntectonic granites may be most strongly developed in plutons that were emplaced within highly ductile host rocks in high-grade terranes such as the amphibolite-facies metasedimentary rocks of the Burwash Formation.

Acknowledgements—The research was financed by a SNORCLE Lithoprobe University Supporting Geoscience Grant awarded to K. B. and W. R. Roest, and by a research contract with the Department of Indian Affairs and Northern Development (DIAND) awarded to K. B. The field work was facilitated by logistical support from the Geological Survey of Canada (GSC) through the Slave Province NATMAP program, and from DIAND. The GSC provided financial support for N. M. Ham while doing field work. G. J. Borradaile is gratefully acknowledged for access to the rock magnetics facilities at Lakehead University. Thanks to W. Padgham for hospitality in Yellowknife and to W. K. Fyson for discussions on the regional geology and granites in general. Journal reviewers B. Housen and B. Tikoff provided insightful comments that significantly improved the paper. This is Lithoprobe contribution no. 908 and DIAND contribution no. 97-009.

REFERENCES

Aranguren, A., Cuevas, J. and Tubía, J. M. (1996) Composite magnetic fabrics from *S–C* mylonites. *Journal of Structural Geology* **18,** 863–869.

Arbaret, L., Diot, H., Bouchez, J. L., Lespinasse, P. and de Saint-Blanquat, M. (1997) Analogue 3D simple-shear experiments of magmatic biotite subfabrics. In *Granite: from segregation of melt to emplacement fabrics*, eds J. L. Bouchez, D. H. W. Hutton and W. E. Stephens, pp. 129–143. Kluwer Academic Publishers, Dordrecht.

Barbarin, B. (1990) Granitoids: main petrogenetic classifications in relation to origin and tectonic setting. *Geological Journal* **25,** 227–238.

Benn, K. (1994) Overprinting of magnetic fabrics in granites by small strains: numerical modelling. *Tectonophysics* **233,** 153–162.

Benn, K., Genkin, M., van Staal, C. R. and Lin, S. (1993) Structure and anisotropy of magnetic susceptibility of the Rose Blanche Granite, southwestern Newfoundland: kinematics and relative timing of emplacement. In *Current Research, Part D, Paper 93-1D*, pp. 73–82. Geological Survey of Canada, Ottawa.

Benn, K., Horne, R. J., Kontak, D. J., Pignotta, G. and Evans, N. G. (1997) Syn-Acadian emplacement model for the South Mountain Batholith, Meguma Terrane, Nova Scotia: Magnetic fabric and structural analyses. *Geological Society of America Bulletin* **109,** 1279–1293.

Blanchard, J. P., Boyer, P. and Gagny, C. (1979) Un nouveau critère de sens de mise en place dans une caisse filonienne: le 'pincement' des minéraux aux épontes. *Tectonophysics* **53,** 1–25.

Bleeker, W. (1996) Thematic structural studies in the Slave Province, Northwest Territories: the Sleepy Dragon Complex. In *Current Research, Part C*, pp. 37–48. Geological Survey of Canada, Ottawa.

Bleeker, W. and Beaumont-Smith, C. (1995) Thematic structural studies in the Slave Province: preliminary results and implications for the Yellowknife Domain, Northwest Territories. In *Current Research. Part C*, pp. 87–96. Geological Survey of Canada, Ottawa.

Bleeker, W., Davis, B. and Villeneuve, M. (1997a) The Slave Province: evidence for contrasting crustal domains and a complex, multistage tectonic evolution (Abstract). In *SNORCLE Transect and Cordilleran Tectonics Workshop Meeting, Lithoprobe Report No. 56*, eds F. Cook and P. Erdmer, pp. 36–37. University of Calgary.

Bleeker, W., Villeneuve, M. and Bethune, K. (1997b) Thematic structural studies in the Slave Province, Northwest Territories: contrasting basement/cover relationships on the western and southwestern flanks of the Sleepy Dragon Complex. In *Current Research Part C*, pp. 27–37. Geological Survey of Canada, Ottawa.

Borradaile, G. J. (1988) Magnetic susceptibility, petrofabrics and strain. *Tectonophysics* **156,** 1–20.

Borradaile, G. J. and Henry, B. (1997) Tectonic applications of magnetic susceptibility and its anisotropy. *Earth-Science Reviews* **42,** 49–93.

Borradaile, G. J. and Werner, T. (1994) Magnetic anisotropy of some phyllosilicates. *Tectonophysics* **235,** 223–248.

Bouchez, J. L. (1997) Granite is never isotropic: an introduction to AMS studies of granitic rocks. In *Granite: From Segregation of Melt to Emplacement Fabrics*, eds J. L. Bouchez, D. H. W. Hutton and W. E. Stephens, pp. 95–112. Kluwer Academic, Dordrecht.

Bouchez, J. L. and Benn, K. B. (1997) Fabrics of granite plutons: bases for their interpretation in terms of emplacement. *Geological Association of Canada Annual Meeting (Abstracts)* **22,** A–15.

Bouchez, J. L., Gleizes, G., Djouadi, T. and Rochette, P. (1990) Microstructure and magnetic susceptibility applied to emplacement kinematics of granites: the example of the Foix pluton (French Pyrenees). *Tectonophysics* **184,** 157–171.

Clarke, D. B. (1981) The mineralogy of peraluminous granites: a review. *Canadian Mineralogist* **19,** 3–17.

Cruden, A. R. and Launeau, P. (1994) Structure, magnetic fabric and emplacement of the Archean Lebel Stock, SW Abitibi Greenstone Belt. *Journal of Structural Geology* **16,** 677–691.

Day, R., Fuller, M. and Schmidt, V. A. (1977) Hysteresis properties of titanomagnetites: grain-size and compositional dependence. *Physics of the Earth and Planetary Interiors* **13,** 260–267.

Fowler, T. K. F. Jr and Paterson, S. R. (1997) Timing and nature of magmatic fabrics from structural relations around stoped blocks. *Journal of Structural Geology* **19,** 209–244.

Fyson, W. K. and Helmstaedt, H. (1988) Structural patterns and tectonic evolution of supracrustal domains in the Archean Slave Province, Canada. *Canadian Journal of Earth Sciences* **25,** 301–315.

Gapais, D. (1989) Shear structures within deformed granites: mechanical and thermal indicators. *Geology* **17,** 1144–1147.

Gleizes, G., Nédélec, A., Bouchez, J. L., Autran, A. and Rochette, P. (1993) Magnetic susceptibility of the Mont-Louis Andorra ilmenite-type granite (Pyrenees): a new tool for the petrographic characterization and regional mapping of zoned granite plutons. *Journal of Geophysical Research* **98,** 4317–4331.

Heider, F., Dunlop, D. J. and Sugiura, N. (1987) Magnetic properties of hydrothermally recrystallized magnetite crystals. *Science* **236,** 1287–1290.

Heider, F., Zitzelsberger, A. and Fabian, K. (1996) Magnetic susceptibility and remanent coercive force in grown magnetite crystals from 0.1 μm to 6 mm. *Physics of the Earth and Planetary Interiors* **93,** 239–256.

Henderson, J. B. (1981) Archean basin evolution in the Slave Province, Canada. In *Precambrian Plate Tectonics*, ed. A. Kroner, pp. 213–235. Elsevier, Amsterdam.

Henderson, J. B. (1985) *Geology of the Yellowknife–Hearne Lake Area, District of Mackenzie: A Segment Across an Archean basin*. Geological Survey of Canada Memoir 414, Ottawa.

Housen, B. A., Richter, C. and van der Pluijm, B. A. (1993) Composite magnetic anisotropy fabrics: experiments, numerical models, and implications for the quantification of rock fabrics. *Tectonophysics* **220,** 1–12.

Ildefonse, B., Arbaret, L. and Diot, H. (1997) Rigid particles in simple shear flow: is their preferred orientation periodic or steady-state? In *Granite: From Segregation of Melt to Emplacement Fabrics*, eds J. L. Bouchez, D. H. W. Hutton and W. E. Stephens, pp. 177–185. Kluwer Academic, Dordrecht.

James, D. T. and Mortensen, J. K. (1992) An Archean metamorphic core complex in the southern Slave Province: basement–cover relations between the Sleepy Dragon Complex and the Yellowknife Supergroup. *Canadian Journal of Earth Sciences* **29,** 2133–2145.

Jamison, W. R. (1991) Kinematics of compressional fold development in convergent wrench terranes. *Tectonophysics* **190,** 209–232.

Kretz, R., Loop, J. and Hartree, R. (1989) Petrology and Li–Be–B geochemistry of muscovite–biotite granite and associated pegmatite near Yellowknife, Canada. *Contributions to Mineralogy and Petrology* **102,** 174–190.

Kusky, T. M. (1989) Accretion of the Archean Slave Province. *Geology* **17,** 63–67.

Kusky, T. M. (1990) Evidence for Archean ocean opening and closing in the southern Slave Province. *Tectonics* **9,** 1533–1563.

Leblanc, D., Gleizes, G., Roux, L. and Bouchez, J. L. (1996) Variscan dextral transpression in the French Pyrenees: new data from the Pic des Trois-Seigneurs granodiorite and its country rocks. *Tectonophysics* **261,** 331–345.

Mahood, G. A., Nibler, G. E. and Halliday, A. N. (1996) Zoning patterns and petrological processes in peraluminous magma chambers: Hall Canyon pluton, Panamint Mountains, California. *Geological Society of America Bulletin* **108,** 437–453.

Olivier, P., de Saint, Blanquat M., Gleizes, G. and Leblanc, D. (1997) Homogeneity of granite fabrics at metre and dekametre scale. In *Granites: From Segregation of Melt to Emplacement Fabrics*, eds J. L. Bouchez, D. Hutton and W. E. Stephens, pp. 113–127. Kluwer Academic, Dordrecht.

O'Reilly, W. (1984) *Rock and Mineral Magnetism*. Blackie and Sons Ltd., Glasgow.

Paterson, S. R. and Tobisch, O. T. (1988) Using pluton ages to date regional deformations: Problems with commonly used criteria. *Geology* **16,** 1108–1111.

Paterson, S. R., Vernon, R. H. and Tobisch, O. T. (1989) A review of criteria for the identification of magmatic and tectonic foliations in granitoids. *Journal of Structural Geology* **11,** 349–363.

Paterson, S. R. and Miller, R. B. (1998) Stoped blocks in plutons: paleo-plumb bobs, viscometers, or chronometers? *Journal of Structural Geology* **20,** 1261–1272.

Pavlis, T. L. (1996) Fabric development in syn-tectonic intrusive sheets as a consequence of melt-dominated flow and thermal softening of the crust. *Tectonophysics* **253,** 1–31.

Riller, U., Cruden, A. R. and Schwerdtner, W. M. (1996) Magnetic fabric and microstructural evidence for a tectono-thermal overprint of the early Proterozoic Murray pluton, central Ontario, Canada. *Journal of Structural Geology* **18,** 1005–1016.

Rochette, P. (1994) Comment on "Magnetic fabrics, crystallographic preferred orientation, and strain of progressively deformed metamorphosed pelites in the Helvetic zone of the Central Alps (Quartenschiefer Formation)" by C. Richter, L. Ratschbacher, and W. Frisch. *Journal of Geophysical Research* **99,** 21,825–21,827.

Rochette, P., Jackson, M. and Aubourg, C. (1992) Rock magnetism and the interpretation of anisotropy of magnetic susceptibility. *Reviews of Geophysics* **30,** 209–226.

Tarling, D. H. and Hrouda, F. (1993) *The Magnetic Anisotropy of Rocks*. Chapman and Hall, London.

Tikoff, B. and Teyssier, C. (1994) Strain and fabric analyses based on porphyroclast interaction. *Journal of Structural Geology* **16,** 477–491.

Tobisch, O. T. and Cruden, A. R. (1995) Fracture-controlled magma conduits in an obliquely convergent continental magmatic arc. *Geology* **23,** 941–944.